Computers and Concrete, Vol. 4, No. 4 (2007) 285-298
DOI: http://dx.doi.org/10.12989/cac.2007.4.4.285

IBEM analyses on half-cell potential measurement for NDE of rebar corrosion

Je-Woon Kyung†

Department of Architectural Environmental Engineering, Hanyang University, 7 Haengdang-dong, Seongdong-gu, Seoul, 133-791, Korea

Sung-Ho Tae‡ and Han-Seung Lee

School of Architecture & Architectural Engineering, Hanyang University, 1271, Sa-1dong, SangNokgu, Ansan, Gyunggido, 425-791, Korea

Yalcin Alver

Graduate School of Science and Technology, Kumamoto University, Kumamoto, Japan

Jo-Hyeong Yoo

Department of Architectural Environmental Engineering, Hanyang University, Ansan, Korea

(Received November 16, 2006, Accepted August 7, 2007)

Abstract. Corrosion of Reinforcement (rebar) is nondestructively estimated by the half-cell potential measurement. As is the case with other nondestructive testings (NDT), understanding of the underlying principles should be clarified in order to obtain meaningful results. Therefore, the measurement of potentials in concrete is analytically investigated. The effect of internal defects on the potentials measured is clarified numerically by the boundary element method (BEM). Thus, a simplified inversion by BEM is applied to convert the potentials on concrete surface to those on rebars, taking into account the concrete resistivity. Because the potentials measured on concrete surface are so sensitive to moisture content, concrete resistivity and surface condition, an inverse procedure to convert the potentials on concrete surface into those on rebars is developed on the basis of BEM. It is found that ASTM criterion is practically applicable to estimate corrosion from the potential values converted. In experiments, an applicability of the procedure is examined by accelerated corrosion tests of reinforced concrete (RC) slabs. For practical use, the procedure is developed where results of IBEM are visualized by VRML (Virtual Reality modeling Language) in three-dimensional space.

Keywords: NDE; inversion by boundary element method (IBEM); half-cell potential; corrosion; concrete resistivity; VRML (Virtual Reality modeling Language).

† Corresponding Author, E-mail: jwkyung@hanyang.ac.kr
‡ E-mail: jnb55@hanyang.ac.kr

1. Introduction

In the past decades, corrosion problems of reinforced concrete structures by salt attack have been widely reported through-out the world. Not only the durability problem, but also the economic impact becomes a major concern (Cederquist 1999, FHWA 1999-2001, Committee Cost of Corrosions 2001, Maurel 2005). Basically, concrete provides a good durable condition for embedded steel with high alkaline environment by forming a passive film on the surface of rebar. Rebars in concrete are chemically protected from corrosion by alkaline environment of concrete. Corrosion is, however, one of the major problems facing engineers today (Emmons and Vaysburd 1997, Kyung, *et al.* 2006). Because concrete is a porous material, carbon dioxide and chloride can penetrate into it. As a result, the passivity of the steel is destroyed, and then rebars in concrete are corroded. The expansion of corrosion products generates cracks which result in serious defects in reinforced concrete (RC) structures. Thus, nondestructive evaluation (NDE) for corrosion of rebars is to be performed in advance to visible inspection of cracking (Dubravka, *et al.* 2000, Ohtsu 2003). So far, two nondestructive techniques of the half-cell potential and the polarization resistance are practically available. The half-cell potential provides information on the probability of corrosion, while the polarization resistance is associated with information on the corrosion rate (Ohsiro, *et al.* 1991, Elsener, 2001, Andrade and Alonso 2001).

For the half-cell potential measurement, the criterion to estimate the probability of corrosion has been already coded in ASTM C876 (1991). It is reported, however, that the potentials measured are too sensitive to moisture content, thickness of concrete cover, surface coating, resistivity of concrete and so forth (Misra and Uomoto 1990). Consequently, the estimation of corrosion by the ASTM criterion is still inconclusive.

An essential drawback of the half-cell potential measurement results from the fact that the potentials are measured not near rebars but on concrete surface. One compensation is to measure the potentials as close to rebars as that probes of the electrode are embedded in concrete or are inserted into the bottom of bore holes (Tamura, *et al.* 1992, Hietpas, *et al.* 2005). Another compensation is to determine the potentials around rebars analytically. Potential distribution and current flow during corrosion process can be formulated by numerical techniques such as the finite element method (FEM), the finite difference method (FDM) and the boundary element method (BEM) (Otomaru 1990, Jaggi, *et al.* 2001, Kranc and Sagues 2001, Kobayashi and Miyagawa 2001). BEM analysis seems to be the most effective for a corrosion problem, because the quantities only on the surfaces are of concern (Aoki, *et al.* 1990).

2. Theory

2.1. Half-cell potential measurement

In the half-cell potential measurement, electric potential u in domain D (concrete) is measured at the surface. The potentials in concrete satisfies the following Laplace equation,

$$\nabla^2(u/R) = 0 \quad \text{in } D \tag{1}$$

where ∇ is the gradient (nabla) operator and R is the concrete resistivity.

In a homogeneous body, R is constant and Eq. (1) becomes,

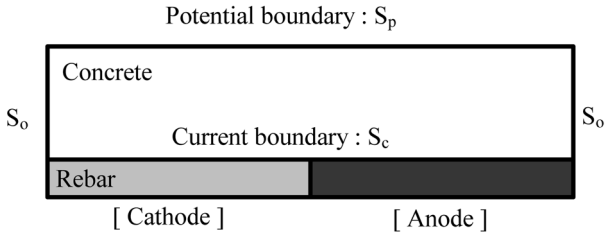

Fig. 1 Boundary conditions of concrete under corrosion in RC

$$\nabla^2 u = 0 \quad \text{in } D \tag{2}$$

As shown in Fig. 1, the boundary of concrete is classified into boundaries S_p, S_o and S_c. Concrete surface, where potentials are measured, corresponds to the potential boundary S_p. Another surface S_o is electrically free where outward flow of the current is equal to zero. The other is the current boundary S_c, which actually represents the interface between concrete and rebar, consisting of the anode region and the cathode region. These boundary conditions are given,

$$u = E(C.S.E) \quad \text{on } S_p \tag{3}$$

$$\frac{\partial}{\partial n}(u/R) = 0 \quad \text{on } S_o \tag{4}$$

$$\frac{\partial}{\partial n}(u/R) = f \quad \text{on } S_c \tag{5}$$

Here the potentials, E, are measured by utilizing a copper-copper sulfate half-cell electrode (*C.S.E.*), and n is the outward normal vector to the surface.

2.2. Boundary element method and inversion by boundary element method

Provided that the concrete is referred to as homogeneous, solution $u(x)$ at point x can be solved by BEM (Brebbia 1978) as.

$$\frac{1}{2}u(x) = \int_S \left[G(x,y)\frac{\partial u}{\partial n}(y) - \frac{\partial G}{\partial n}(x,y)u(y) \right] dS \tag{6}$$

where $S = S_p + S_o + S_c$ and points y are located on the boundary S surrounding the domain D.

$G(x, y)$ is the fundamental solution, as follows;

$$G(x,y) = \frac{1}{4\pi r} \quad \text{in the three-dimensional (3-D) body} \tag{7}$$

$$G(x,y) = \frac{1}{2\pi} \ln\left(\frac{1}{r}\right) \quad \text{in the two-dimensional (2-D) body} \tag{8}$$

Here r is the distance between x and y. The boundary is discretized into boundary meshes, prescribing potential u_j and current $\frac{\partial u_j}{\partial n}$ at point x_j on a boundary mesh. Then, a set of linear algebraic equations are obtained,

$$\sum_{j=1}^{N}\left\{\frac{\delta_{ij}}{2}-\frac{\partial G_{ij}}{\partial n}\right\}(u_j)=\sum_{j=1}^{N}\{G_{ij}\}\left\{\frac{\partial u_j}{\partial n}\right\}, \qquad (i=1,N) \tag{9}$$

where N is the number of boundary meshes, δ_{ij} is Kronecker's delta symbol and G_{ij} is the digitized fundamental solution for points x_i and x_j.

In the BEM, internal potentials $u(x)$ are determined by,

$$u(x)=\int_{S_c} G(x,y)\left(\frac{\partial u}{\partial n}(y)\right)dS-\int_{S_p}\left(\frac{\partial G}{\partial n}(x,y)\right)u(y)dS \tag{10}$$

Applying Eq. (10) to an inverse analysis, the points x_i, which are actually located at the interface with the rebars, are referred to as internal points. Thus, the current boundary S_c is neglected because $\partial u/\partial n(y)$ is always equal to zero, and the potential boundary S_p is only taking into account. Then, Eq. (10) is digitized as,

$$u_i=\sum_{j=1}^{M}\left[-\frac{\partial G_{ij}}{\partial n}\right]u_j\Delta S \tag{11}$$

As shown in Fig. 2, the surface of concrete to be measured is divided into M rectangular elements of area ΔS. In an experiment, measuring point x_j at the center of the element is marked and potential is measured. Potentials at the interface with the rebars, u_i, are computed as internal potentials, substituting potentials u_j and area ΔS into Eq. (11).

The procedure is so simple as to be readily implemented in a microcomputer. Hereinafter, the potentials at the interface with the rebars are referred to as those on the rebars. To take into account the concrete resistivity, Eq. (11) is converted as,

$$u_i=\sum_{j=1}^{M}\left[-\frac{\partial G_{ij}}{\partial n}R\right]u_j\Delta S \tag{12}$$

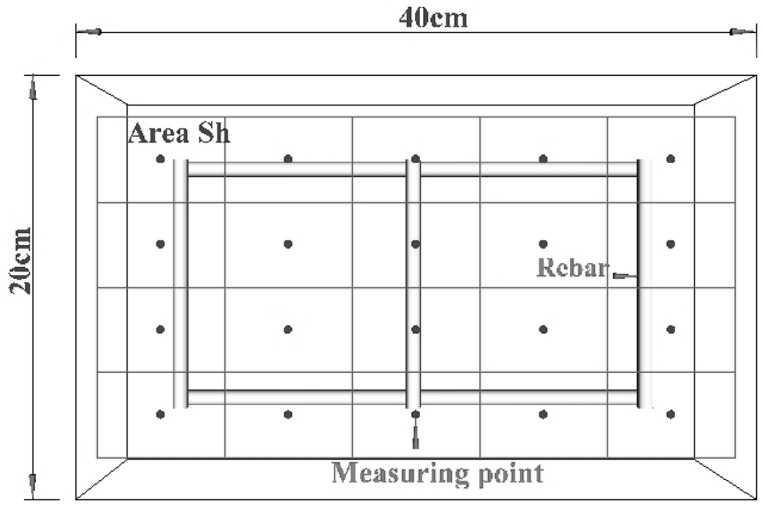

Fig. 2 Configuration of the half-cell potential measurement

Here R is the relative coefficient of concrete resistivity. When a void and a determination are identified by radar measurement,

$$R = \frac{R_{nv}}{R_v} \tag{13}$$

where R_{nv} is the averaged concrete resistivity of intact part and R_v is that of void part. In the case that distribution of the resistivity is fairly inhomogeneous,

$$R = \frac{R_{ave}}{R_p} \tag{14}$$

where R_{ave} is the averaged concrete resistivity of the surface and R_p is the resistivity at each location.

The method to convert the half-cell potential by Eq. (12) is named the inversion by BEM (IBEM).

3. Experiment

3.1. Simulation analysis

A numerical experiment was performed by a model shown in Fig. 3. The concrete blocks of dimension 3 cm × 25 cm and 5 cm × 25 cm were taken into consideration.

The boundary is divided into 42 meshes and the void of 15 cm length, 1 cm width and 1 cm thickness is located from 1 cm to 3 cm below the top surface. In the analysis, four cases were analyzed to study the effect of defects on the half-cell potential measurement. Two cases are of no void with different depths of 3 cm and 5 cm. Another two cases contain the void 1 cm below the top surface with 3 cm beam depth and 2 cm below it with 5 cm depth. As shown in Fig. 3, potential were given at the bottom boundary as -0.1V at the anode region and +0.1V at the cathode region. To clarify the effect of the void, the offset potential was not taken into consideration. By conducting BEM analysis, potentials at the top surface were determined. Results are shown in Fig. 4 and Fig. 5. It is found that potentials at the top surface are amplified due to the presence of the void. It implies that potentials more negative could be measured by the half-cell potential measurement in the case that the void exists inside the concrete cover. Comparing two cases of voids in Fig. 4 and Fig. 5, it is known that the effect of a shallow void on the amplification is greater than that of a deep void.

From these potentials at the top surface, the potentials at the bottom boundary (Fig. 3) corresponding to

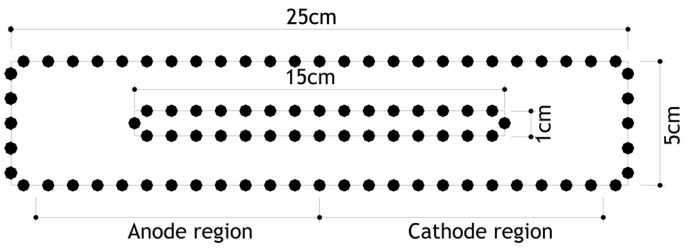

Fig. 3 BEM model containing a void of 15 cm length and 1 cm width

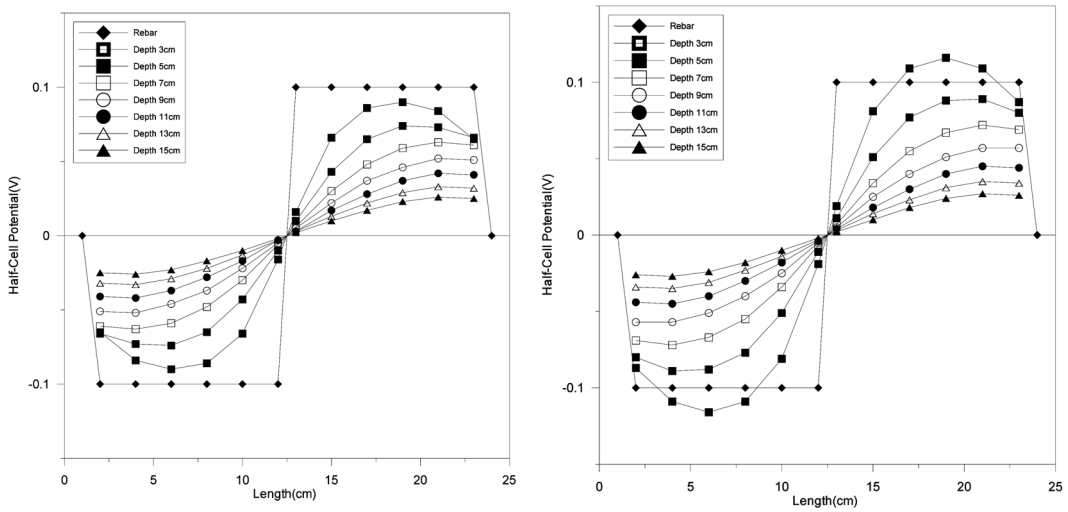

(a) Potentials at the top surface by BEM (b) Solutions by IBEM from the potentials by BEM

Fig. 4 Potentials at the top surface of intact specimen

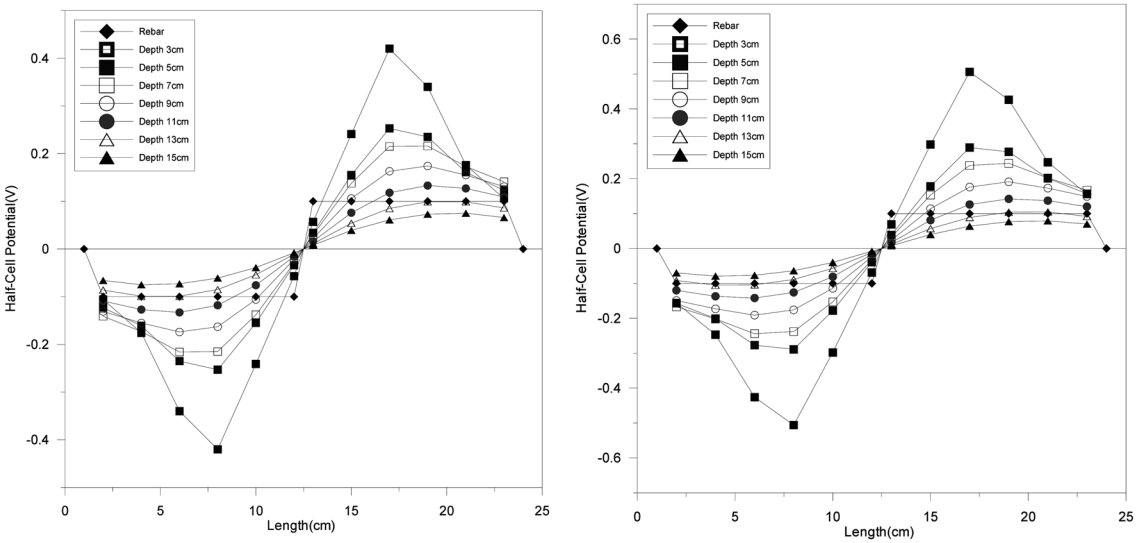

(a) Potentials at the top surface by BEM (b) Solutions by IBEM from the potentials by BEM

Fig. 5 Potentials at the top surface of specimen including voids

the reinforcement were determined by IBEM, only taking into account the potentials at the top surface. Results are shown in Fig. 4 and Fig. 5. In the case of non-void, reasonable agreement with the given potentials is observed. In the case of containing voids, however, potentials determined are amplified as well. It implies that the presence of the void over the reinforcement could mislead to more negative potentials than actual values, even though IBEM analysis is applied.

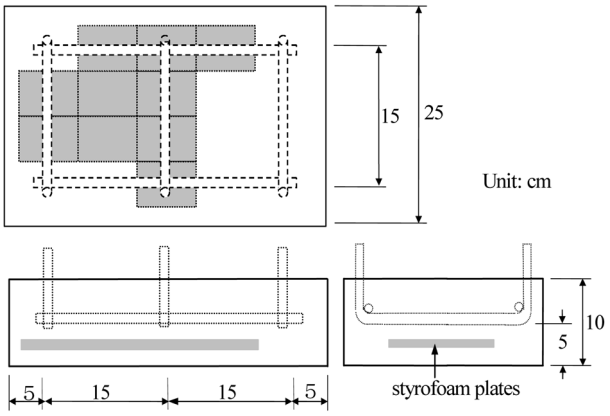

Fig. 6 RC slabs arrangement of rebars and voids

Table 1 Mixture proportion of concrete

Maximum gravel size (mm)	W/C (%)	s/a (%)	Weight for unit volume (kg/m^3)				NaCl/W (%)	Slump (cm)
			Water	Cement	Fine aggregate	Coarse aggregate		
20	50	48	172	344	825	1021	3	8.0

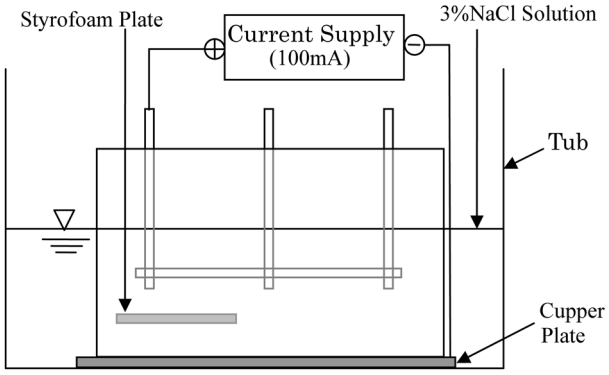

Fig. 7 Accelerated corrosion test

3.2. Accelerated corrosion test

Two types of specimens were cast. One was RC slab of dimension 10 cm × 25 cm × 40 cm. Rebars of 10 mm diameter were embedded at 5 cm cover thickness. The other with the void is of the same dimension. A styrofoam plate of 1 cm thickness was embedded to simulate the void as shown in Fig. 6.

To accelerate corrosion, 3% NaCl solution was mixed. Mixture proportion of concrete is given in Table 1. Uniaxial compressive strength of concrete is 41.45 MPa at 28days. The specimens were moisture-cured at 20°C for 28days. After removal from the mold, the top surface of each specimen and rebar surface out of it were epoxy-coated to protect from corrosion. Rebars in concrete were artificially corroded by an electrolytic corrosion test for 63hrs. A test set-up is shown in Fig. 7. A

copper plate was placed on the bottom of a tub. The specimen was mounted on the copper plate and 3% NaCl solution was filled up to the top surface of the specimen. By using a current supply, constant 100 mA electric current was charged between the rebars and the copper plate.

3.3. Three-dimensional illustration

Visualization procedure has been developed by using VRML. VRML is a real-time interactive program to simulate the virtual model in 3-D graphic. The geometry of concrete structure and corrosion information on the rebar can be entirely displayed in 3-D space.

Such data as coordinates of locations, rebar diameters, rod bar arrangement, cover thickness, polarized resistance, concrete resistance and half-cell potential are denoted. In the case that the geometrical information of rebar inside concrete is not available, other techniques as radar is applicable to estimate the location, size and depth of rebar. According to IBEM analysis, illustration of potentials on the surface of rebars by 2-D might be difficult to distinguish the differences of rebar depths. In this respect, VRML has been introduced as 3-D graphic.

In VRML display, rebar arrangement is categorized as the type of rod arrangement. Based on results measured, corrosion degrees of rebars are classified. Thus, the development of VRML for visualizing the corrosion information is performed (Kyung, *et al.* 2005).

4. Results

4.1. Resistivity measurement

As shown in Figs. 4 and 5, in the case of containing void, potentials determined are amplified. To compensate the specimen containing a void, the concrete resistivity is measured as well as the half-cell potential by a portable corrosion monitoring system (Shikoku Research Institute Inc.) in Fig. 8.

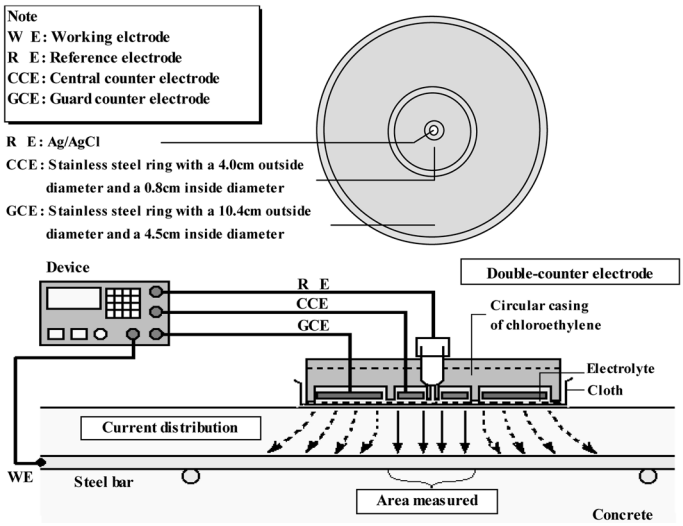

Fig. 8 Measurement using a double-counter electrode

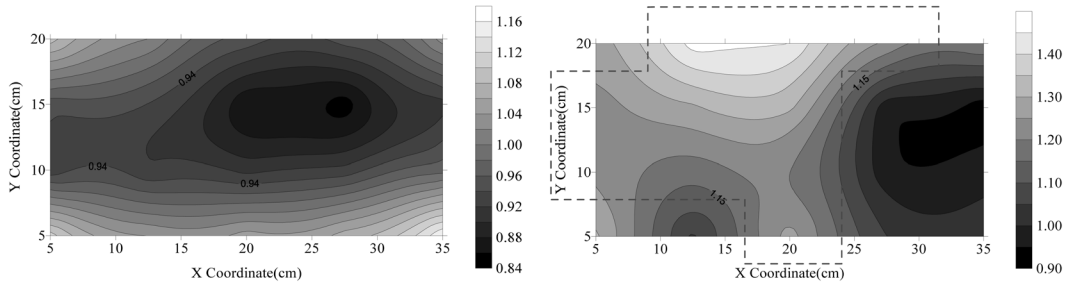

(a) Intact slab (b) Slab including void

Fig. 9 Concrete resistivity at 63Hr (kΩ)

Table 2 Relative coefficients of concrete resistivity in intact specimen : R_{ave}= 0.982kΩ

No.	1	3	5	7	9	11	13
R_p	1.110	1.050	1.160	0.923	0.927	0.948	0.863
R	1.130	1.069	1.181	0.939	0.944	0.965	0.878

Table 3 Relative coefficients of concrete resistivity

	0Hr	24Hrs	48Hrs	54Hrs	63Hrs
R_p	3.273	1.777	1.295	1.184	1.074
R	3.328	2.175	1.538	1.390	1.287

In the two types of specimens, the concrete resistivity was measured at 20 points, of which locations are clearly denoted in Fig. 2. As shown in Fig. 9(a), the intact slab was measured at 63 hrs elapsed in the electrolytic test. It is found that variation of the concrete resistivity were fairly small on the concrete surface. A result of the void specimen is shown in Fig. 9(b). The concrete resistivity of void part is higher than that of non-void part. Comparing these two parts, averaged values of concrete resistivity are shown in Table 2 and Table 3. Thus, half-cell potentials on rebars were compensated by IBEM using the concrete resistivity in Table 2 and Table 3. In this case, coefficient of concrete resistivity, R, is calculated by Eqs. (12) and (13). In the case of non-void, the average value R_{ave} is equal to 0.982 kΩ. Thus, half-cell potentials on rebars were compensated by using the concrete resistivity in Table 2. The relative coefficient R is determined a shown in Table 2 based on Eq. (14).

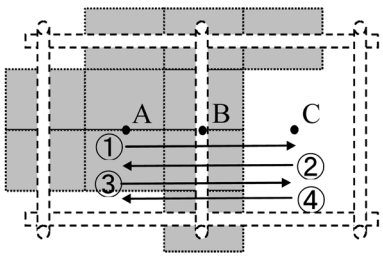

Fig. 10 Radar measurement

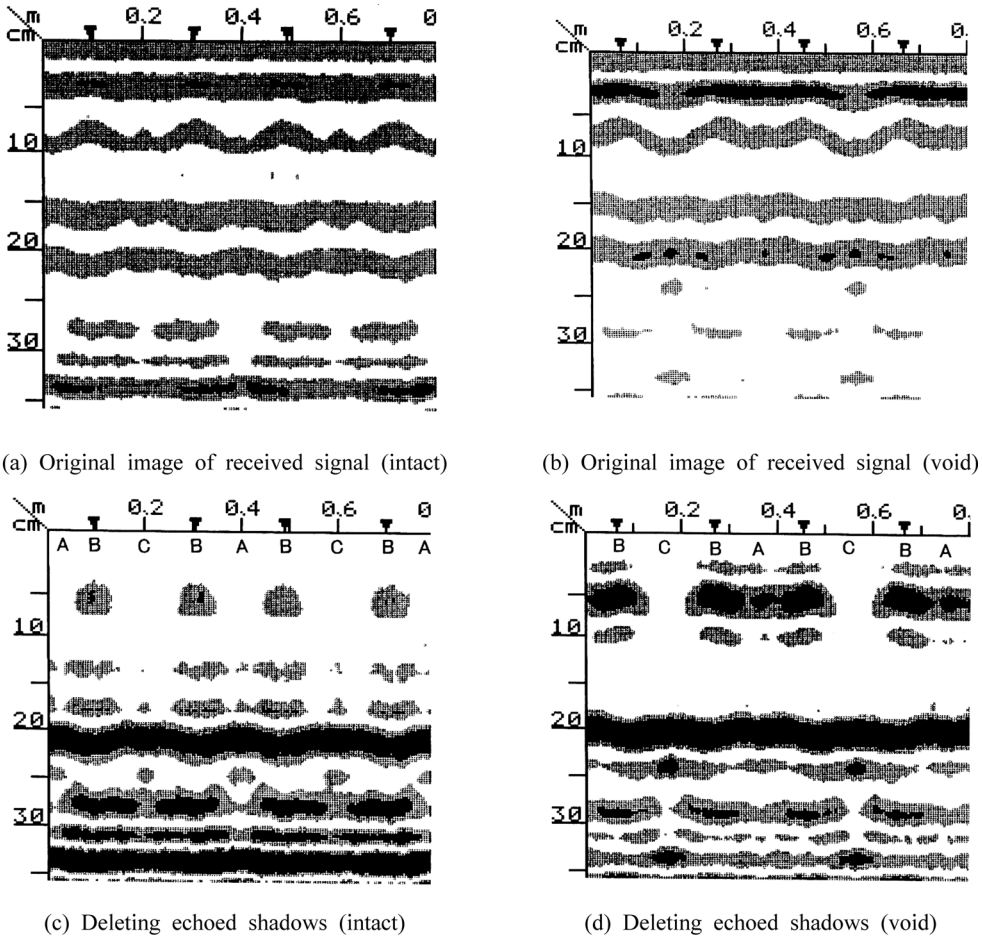

(a) Original image of received signal (intact)

(b) Original image of received signal (void)

(c) Deleting echoed shadows (intact)

(d) Deleting echoed shadows (void)

Fig. 11 Radar measuring results

4.2. Radar measurement

Simulating in situ observation, locations of rebars and voids were determined by employing the radar system (RC Radar, Japan Radio Co, LTD.) in the two specimens of non-void and void. Radar antenna is scanned from A to C (① and ③) two times and from C to A (② and ④) two times as shown in Fig. 10. Results are given in Fig. 11. Original images from received signals are shown in Fig. 11(a) and (b). Here, the depth is measured from the bottom surface of the specimen, and the depths of the rebars are 5 cm. Because of various reflected waves, many shaded zones are observed. Deleting echoed shadows, the locations of rebar at approximate 5 cm depth are clearly identified in Fig. 11(c). In Fig. 11(d), it is found that the locations of rebar at approximate 5 cm depth and of voids at approximate 2 cm depth. It is bound that the discrepancy between the arrangement of rebars in design and the actual locations is within a few millimeters.

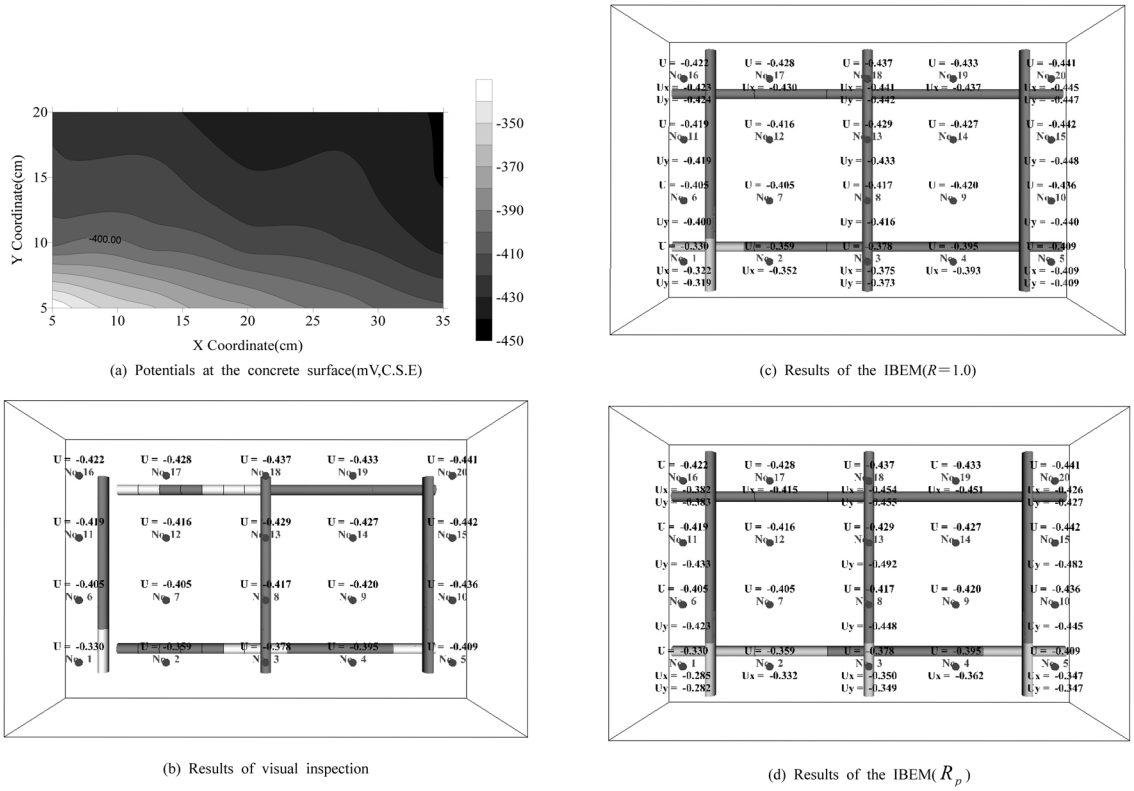

Fig. 12 Half-cell potential result on intact slab

Table 4 Criterion for half-cell potential (mV vs. CSE) based on ASTM C876

Potential value	Criterion	Color of rebars
-200 mV < E	No corrosion	White
-350 mV < $E \leqq$ -200 mV	Uncertain	Orange
$E \leqq$ -350 mV	Active corrosion	Red

4.3. Half-cell potential measurement

Half-cell potentials were measured at 20 points as shown in Fig. 2. Contour map of the potentials observed in the intact RC slab measured at 63 hrs elapsed are given in Fig. 12(a). According to the ASTM criterion, potentials more negative than -350 mV (C.S.E) indicate very high probability (more than 90%) of active corrosion. The potentials between -200 mV and -350 mV imply uncertainty on corrosion. The potentials less negative than -200mV suggest high probability of no corrosion. Criterion for half-cell potential is giver in Table 4. After the potential measurement, the specimens were broken and the rebars were removed to identify the corroded area. Results are shown Fig. 12(b). By applying Eq. (9), potential at rebars were computed and then the ASTM criterion was applied to the potentials at the rebars. Results are given in Fig. 12(c). Reasonable agreement between the actual corroded region and the estimated is observed.

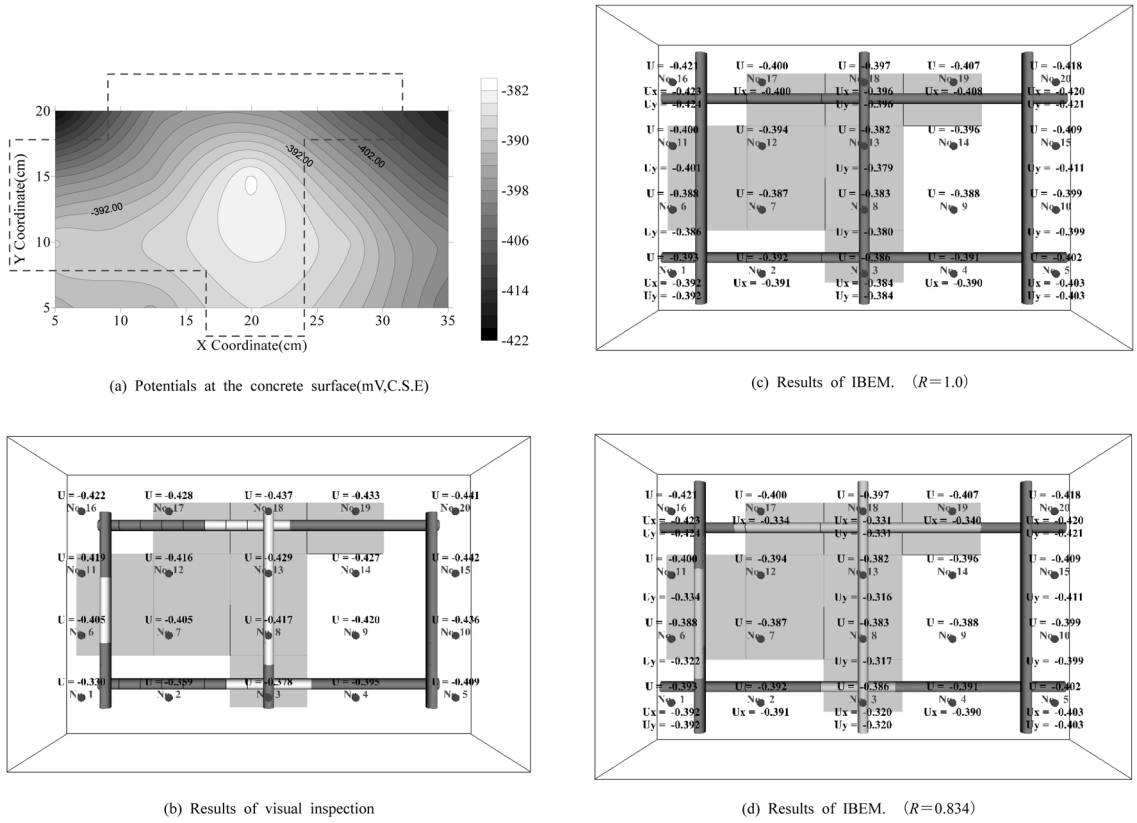

(a) Potentials at the concrete surface(mV,C.S.E)

(c) Results of IBEM. (R=1.0)

(b) Results of visual inspection

(d) Results of IBEM. (R=0.834)

Fig. 13 Half-cell potential result on slab including void

Result of potentials on the surface in the case including the void is given in Fig. 13(a). It suggests that all portions of rebars are corroded because all are lower than -350 mV. The specimen was broken and the rebars were removed to identify the corroded area. Results are shown Fig. 13(b). By applying Eq. (10), potentials at rebars were determined by employing relative coefficients of the concrete resistivity in Table 2 and then the ASTM criterion was applied to the potentials at the rebars. Results are given in Fig. 13(c). Good agreement between both actual and estimated corroded regions is observed.

Since the procedure for compensation could provide direct information on the potentials at the rebar, it can be applied to identify corroded regions of the rebar precisely. Thus, a reliable procedure to identify corroded regions of rebars is developed.

5. Conclusions

A compensation procedure for the half-cell potential measurement is studied and the IBEM analysis is developed. The procedure converts the potentials on concrete surface to those on rebars or at the interface with rebars. The applicability is examined by a numerical analysis and accelerated corrosion tests of RC slab. Results obtained are summarized, as follows:

(1) By BEM analysis, potentials at the top surface were determined. It is found that potentials at

the top surface are amplified due to the presence of the void. It implies that potentials more negative could be measured by the half-cell potential measurement in the case that the void exists inside the concrete cover.

(2) By IBEM analysis, the potentials at rebars were computed, to which the ASTM criterion was applied to the estimation of corrosion. Good agreement between predicted corrosive region of rebars and actually corroded region is observed in the intact specimen.

(3) In the case of the specimen with a void, it is confirmed that the half-cell potential measurement misleads to more negative values than the actual potentials of the reinforcement. It is found that concrete resistivity of void part is higher than that of no void part.

(4) The procedure is improved, taking into account the effect of the void on the concrete resistivity. The applicability of the procedure is confirmed in the experiment of RC slab with a void. Thus, a reliable procedure to identify corroded region of rebars is developed.

Acknowledgements

This work was supported by Sustainable Building Research Center Hanyang University which was supported the Engineering Research Center program of Ministry of Science and Technology (#R11-2005-056-04003-0). The work presented in this paper was funded by Center for Concrete Corea(05-CCT-D11), supported by KICTTEP under the MOCT.

References

Andrade, C. and Alonso, C. (2001), "On-site measurements of corrosion rate of reinforcements", *Const. Bldg. Mater.*, **15**(2-3), 141-145.

Aoki, S., Kishimoto, K and Sakata, M. (1990), "Boundary element analysis of galvanic corrosion", *Corrosion Science*, **30**(2-3), 299-311.

ASTM C876 (1991), *Standards Test Method for Half Cell Potentials of Reinforcing Steel in Concrete*.

Brebbia, C. A. (1978), *The Boundary Element Method for Engineers*, Pentech Press Ltd., London.

Cederquist, S. C. (1999), "Repairing america's deteriorating bridges", *Materials Performance*, **38**(5), 20.

Chris, M. and Bruce, C. (1997), *Teach yourself VRML2 in 21 days*, San·net, NY.

Committee on Cost of Corrosion in Japan, (2001), *Report on Cost of Corrosion in Japan*, Japan Society of Corrosion Engineering and Japan Association of Corrosion Control.

Dubravka, B., Dunja, M. and Dalibor, S. (2000), "Non-destructive corrosion rate monitoring for reinforced concrete structures", *Proceedings of 15th WCNDT*, Roma, October.

Emmons, P. H. and Vaysburd, A. M. (1997), "Corrosion protection in concrete repair: myth and reality", *Concrete International*, **19**(3), 47-56.

Elsener, B. (2001), "Half-cell potential mapping to assess repair work on RC structures", *Const. Boldg. Mater.*, **15**(2-3), 133-139.

FHWA (1999-2001), *Corrosion Cost and Preventive Strategies in the United States*, FHWA-RD-01-156.

Hartman, J. (1996), *VRML 2.0 Handbook*, Addison-Wesley, NY.

Jaggi, S., Bohni, H. and Elesner, B. (2001), "Macrocell corrosion of steel in concrete-experiments and numerical modelling", *Proceedings of Eurocorr 2001*, Milan, September-October.

Kobayashi, K. and Miyagawa, T. (2001), "Study on estimation of corrosion rate of reinforcing steel in concrete by measuring polarization resistance", *Proceedings of JSCE*, Kumamoto, October.

Koyama, R., Yajima, T. and Uomoto, T. (1995), "Prediction of steel corrosion by spontaneous potential measurement", *Proceedings of Japan Concrete Institute*, Hiroshima, June.

Kranc, S. C, Sagues, A. A. (2001), "Detailed modeling of corrosion macrocells on steel reinforcing in concrete", *Corrosion Science*, **43**(4), 1355-1372.
Misra, S. and Uomoto, T. (1990), "Corrosion of rebars under different corrosions", *Proceedings of Japan Concrete Institute*, Sapporo, June.
Otomaru, M., Murakami, Y. and Ohtsu, M. (1990), "Half-cell potentials analysis by BEM for corrosion monitoring", *Proceedings of Japan Concrete Institute*, Sapporo, June.
Ohshiro, T., Tanikawa, S. and Goto, N. (1991), "A study on corrosion evaluation of steel reinforcements in concrete" , *Proceedings of Japan Concrete Institute*, Kobe, June.
Ohtsu, M. and Yamamura, H. (1991), "Charge simulation method of half-cell potential for corrosion evaluation", *Proceedings of Japan Concrete Institute*, Kobe, June.
Ohtsu, M. and Yamamoto, T. (1997), "Compensation procedure for half-cell potential measurement", *Construction and Building Material,* **11**(7-8), 395-402.
Tamura, H., Nagayama, M. and Shimozawa, K. (1992), "A case study on reinforcement corrosion in an existing Rc structure", *Proceedings of Japan Concrete Institute*, Nigata, June.
Sung, S. H., Kyung, J. W. and Ujiro, J. (2006), "Service life estimation of concrete structures reinforced with Cr-bearing rebars under macrocell corrosion conditions induced by cracking in cover concrete", *The Iron and Steel Institute of Japan International,* **47**(6), 875-882.
Kyung, J. W., Yokota, M., Leelalerkiet, V. and Ohtsu, M. (2005), "Visual reality presentation for nondestructive evaluation of rebar corrosion in concrete based on inverse BEM", *The Korean Society for Nondestructive Testing,* **25**(3), 157-162.
Hietpas, K., Ervin, B., Banasiak. J., Pointer, D., Kuchma, D. A., Reis, H. and Bernhard, T. (2005), "Ultrasonics and electromagnetics for a wireless corrosion sensing system embedded in structrual concrete", *Smart Struct. Sys.*, **1**(3), 267-282.
Maurel, O. (2005), "Relation between total degradation of steel concrete bond and degree of corrosion of RC beams experimental and computational studies", *Comput. Concrete*, **2**(1), 1-18.

CC